Journal of Applied Polymer Science

# Effect of Cross-Linker on Morphology, Catalytic Activity, and Recyclability of Immobilized Palladium Chloride

**Yong-Guang Jia, Jian Jiang, Ling-Yan Liu, Wei-Xing Chang, Jing Li**
State Key Laboratory of Elemento-Organic Chemistry, The College of Chemistry, Nankai University, Tianjin 300071, China
Correspondence to: L.-Y. Liu (E-mail: liulingyan@nankai.edu.cn) or J. Li (E-mail: lijing@nankai.edu.cn)

**ABSTRACT:** Two kinds of immobilized palladium (Pd) catalysts were prepared by reversible addition fragmentation chain transfer polymerization of pyridine-containing monomer followed by immobilizing palladium chloride ($PdCl_2$) on block copolymers. Namely, one of them includes the cross-linking structure of maleic anhydride with 1,6-diaminohexane (cross-linker), polystyrene-*block*-poly (4-(4-vinylbenzyloxy)butylpicolinate-*alt*-maleic anhydride)-Pd (PS-*b*-P(VBP-*alt*-MAn)-Pd), and the other is its non-cross-linking counterpart, polystyrene-*block*-poly(4-(4-vinylbenzyloxy) butylpicolinate)-Pd (PS-*b*-PVBP-Pd). From transmission electron microscopy images, it could be observed that they both assembled into micelles in the selective solvents. The Pd of PS-*b*-P(VBP-*alt*-MAn)-Pd located in the core of micelles, whereas the Pd of PS-*b*-PVBP-Pd was on the shell of the micelles. The PS-*b*-P(VBP-*alt*-MAn)-Pd can be continuously used for five times without any appreciable loss of activity in the aqueous Suzuki-coupling reaction. However, the catalytic activities of the PS-*b*-PVBP-Pd decreased sharply with the increase in the recycle times. Thus, this promising cross-linking strategy not only greatly restrained the loss of Pd in the catalytic cycles, but also effectively maintained the immobilized Pd catalyst's high activity. © 2012 Wiley Periodicals, Inc. J. Appl. Polym. Sci. 000: 000–000, 2012

**KEYWORDS:** cross-linking; copolymers; morphology; recycling; catalysts

Received 23 May 2012; accepted 30 July 2012; published online
**DOI: 10.1002/app.38417**

## INTRODUCTION

Palladium (Pd) has been demonstrated to be one of the most powerful and versatile catalyst in modern organic synthesis and widely used for a significant number of synthetic transformations.[1] Moreover, water is the most abundant and ecologically benign solvent in nature. Thus, the reactions catalyzed by Pd in water have ignited the scientists' enthusiasm recently. However, with regard to these reactions, the major limit is the difficulty in separating the catalyst from the reaction system and recycling continuously,[2,3] thus resulted in the loss of the expensive and toxic Pd. Furthermore, the final products are frequently contaminated with the residual Pd, especially in the pharmaceutical industry. To overcome these drawbacks and with respect to the green chemistry,[4,5] Pd catalysts are often immobilized on a variety of solid supports such as clay,[6] metal oxides, including silica,[7–11] alumina,[12] zeolites,[13] and also polymers.[14–19] Among these matrices, polymer is an excellent candidate for its highly designable property.

With the development of controlled/living radical polymerization techniques,[20–22] block copolymers have attracted increasing attention due to the ability of readily form organized micellar aggregates with well-defined nanoscopic morphologies.[23] Therefore, more and more functional block copolymers have been used to support Pd catalysts for improving Pd catalysts' properties at the nanometer scale.[24] Up-to-date, ligand-containing block copolymers such as polystyrene-*b*-poly(*m*-vinyltriphenylphosphine),[25] poly(ethyleneglycol)-*b*-poly(4-vinylpyridine),[26] polystyrene-*b*-poly(4-vinylpyridine),[27–31] poly(ethylene oxide)-*b*-poly(2-vinylpyridine),[32] and block copolymer with pendent *N*-heterocyclic carbene[33] have been successfully applied to the immobilization of Pd catalysts. In comparison with phosphine-containing and carbene-containing counterparts, the advantages of pyridine-containing copolymers are mainly on their lower toxicity[28] and easier synthesis. However, the recyclability of these pyridine-supported Pd catalysts still remained a challenge,[19,33,34] even though these catalysts could exhibit similar high activity to their homogenous counterparts. It may be due to the pyridine segments of the copolymers that always assemble into the shell of micelles,[28,35] and a great deal of pyridine groups could not coordinate well with Pd owing to the larger steric hindrance. Consequently, Pd would easily leach from the shell and lose its activity quickly. To avoid the Pd running off as much as possible, the introduction of maleic anhydride

Additional Supporting Information may be found in the online version of this article.

Applied Polymer SCIENCE

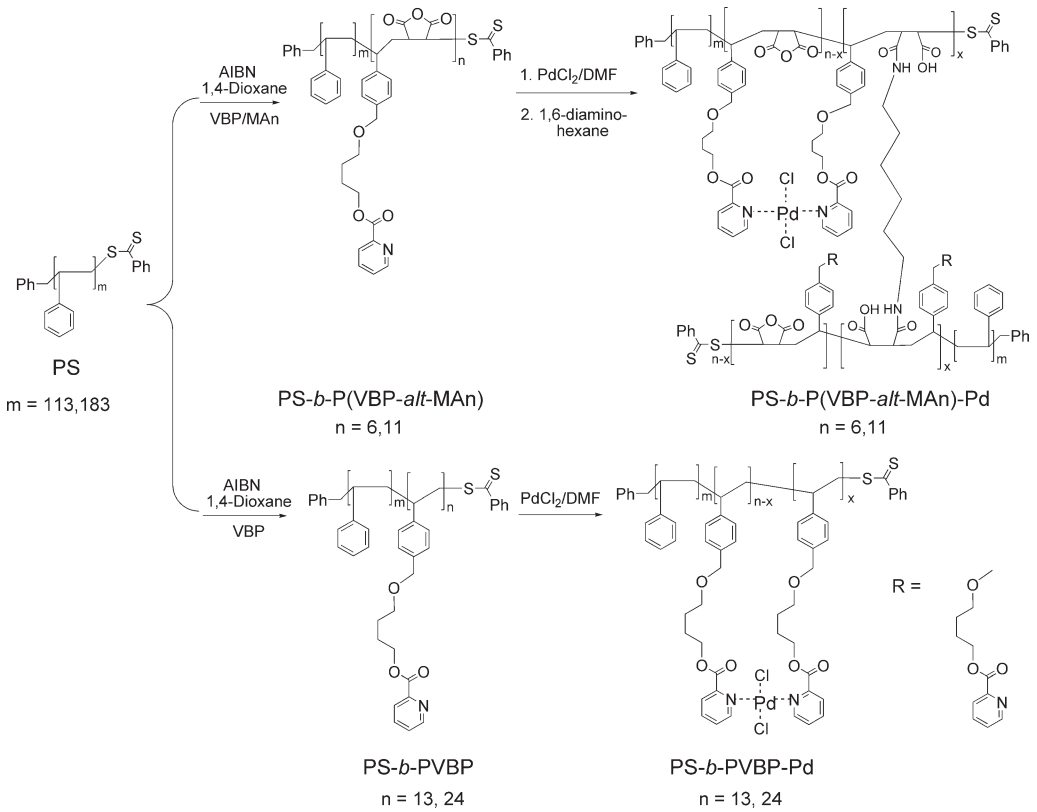


**Scheme 1.** Synthetic scheme showing the structures of the copolymers PS-*b*-P(VBP-*alt*-MAn) and PS-*b*-PVBP as well as the immobilization of palladium chloride. (Note: there is not only the inter-chain but also the intra-chain coordination of pyridine with palladium chloride. More importantly, not all of pyridine groups are involved in the coordination with palladium chloride.)

(MAn) into the polymer backbone was herein intended to cross-link with 1,6-diaminohexane. In our research, this cross-linking could strengthen the preservation of the morphology of Pd catalyst. Simultaneously, a flexible spacer between the backbone and the pyridine groups was also added to reduce the steric hindrance of the coordination between pyridine groups and Pd.

With these in our mind, we developed a new approach for the synthesis of immobilized Pd catalyst based on heterogeneous catalyst system (Scheme 1). The immobilized Pd catalyst was synthesized by reversible addition fragmentation chain transfer (RAFT) copolymerization of 4-(4-vinylbenzyloxy)butylpicolinate (VBP) with MAn followed by coordination of pyridine groups with $PdCl_2$ and cross-linking of MAn units with 1,6-diaminohexane. For comparison, the $PdCl_2$ was also immobilized on the copolymers without MAn units under the same conditions. More importantly, we mainly focused on the effect of cross-linker on the morphology, catalytic activity, and recyclability of these immobilized Pd catalysts in this study.

## EXPERIMENTAL

### Materials

Styrene (J & K Technology Co., Ltd. Acros Organics, Beijin, China) was filtrated through alumina (to remove inhibitors), stirred with $CaH_2$ overnight, and distilled under reduced pressure before use. Azobis(isobutyronitrile) (Tianjin Chemical Company) was recrystallized from methanol twice, and MAn (>99%, Tianjin Guangfu Fine Chemical Research Institute) was recrystallized from $CHCl_3$ twice before use. Benzyl benzodithioate and VBP were synthesized according to the literature.[36,37] Picolinic acid, 4-vinylbenzyl chloride, palladium chloride ($PdCl_2$), iodobenzene, phenylboronic acid, and potassium *tert*-butoxide were purchased from Sigma-Aldrich (Beijin, China). Potassium carbonate, bromomethylbenzene, bromobenzene, carbon disulfide, 1,6-diaminohenxane, and magnesium were used as received (Tianjin Chemical Company). All other common solvents were purified using standard procedures.

### Characterizations

$^1$H-NMR and $^{13}$C-NMR spectra were recorded on a Bruker Avance 400 spectrometer operating at 400 MHz for $^1$H and 100 MHz for $^{13}$C using $CDCl_3$ as the solvent and TMS as the internal standard. Molecular weights and molecular weight distributions were measured on an Agilent Technologies 1200 series gel permeation chromatography (GPC) equipped with a G1362A differential refractive index detector, with THF as eluent at a flow rate 1 mL/min. The instrument was calibrated with monodispersed polystyrenes. Fourier transform infrared spectra were recorded on a Bruker Tensor 27 using KBr pellets for solid samples. Transmission electron microscopy (TEM) images were obtained on a Tecnai G2 20 S-TWIN electron microscope equipped with a Model 794 CCD camera (512 × 512) (gatan) with an accelerating voltage of 200 kV. Sample solutions (0.5

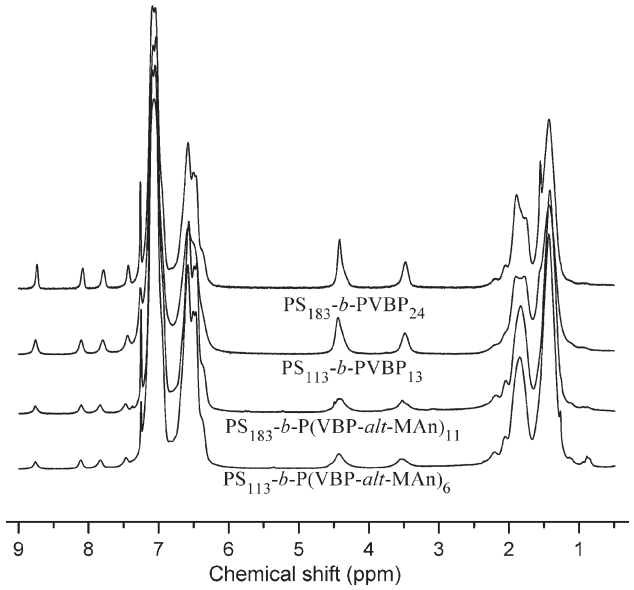


**Figure 1.** $^1$H-NMR spectra of PS-*b*-P(VBP-*alt*-MAn) and PS-*b*-PVBP in $CDCl_3$.

mg/mL in THF/ethanol, 3 : 2, v/v) were dropped onto 300-mesh copper TEM grids and dried for 7 days at room temperature. The Pd contribution was measured by inductive-coupled plasma atomic emission spectrometer (ICP-9000(NtM), Therom Jarrell-Ash Corp). Gas chromatography (GC) analyses were performed on an Agilent 7890-GC instrument. High-resolution mass spectrometry was performed on a Varian QFT-ESI instrument.

## RESULTS AND DISCUSSION

### Synthesis and Characterization of PS-*b*-P(VBP-*alt*-MAn) and PS-*b*-PVBP

Two different molecular weight polystyrenes were used as macroinitiators to reinitiate the mixture of 4-(4-vinylbenzyloxy)butylpicolinate (VBP) and maleic anhydride (MAn) in a molar ratio of 1 : 1 or VBP. As a result, four new different molecular weight diblock copolymers (PS-*b*-P(VBP-*alt*-MAn) and PS-*b*-PVBP) were synthesized. All the resonance peaks of the diblock copolymers could be clearly assigned in the $^1$H-NMR spectra (Figure 1).

**Table I.** Characteristics of PS, PS-*b*-PVBP, and PS-*b*-P(VBP-*alt*-MAn)

| (Co)polymer sample | Conv. (%)[a] | $M_{n,theor}$ ($10^3$)[b] | $M_{n,GPC}$ ($10^3$)[c] | $M_w/M_n$[c] |
|---|---|---|---|---|
| $PS_{113}$ | 56.2 | 12.0 | 10.9 | 1.20 |
| $PS_{183}$ | 46.0 | 19.3 | 17.0 | 1.21 |
| $PS_{113}$-*b*-P(VBP-*alt*-MAn)$_6$ | 22.4 | 14.4 | 13.4 | 1.30 |
| $PS_{183}$-*b*-P(VBP-*alt*-MAn)$_{11}$ | 14.3 | 23.8 | 20.8 | 1.21 |
| $PS_{113}$-*b*-$PVBP_{13}$ | 21.1 | 16.4 | 14.6 | 1.29 |
| $PS_{183}$-*b*-$PVBP_{24}$ | 19.4 | 26.7 | 24.7 | 1.24 |

[a]Calculated by $^1$H-NMR.
[b]Theoretical molecular weight ($M_{n,theor}$) = $[M_0]/[RAFT]_0$ × conversion % × molecular weight ($M_W$) of monomer + $M_W$ of RAFT.
[c]Determined by GPC.

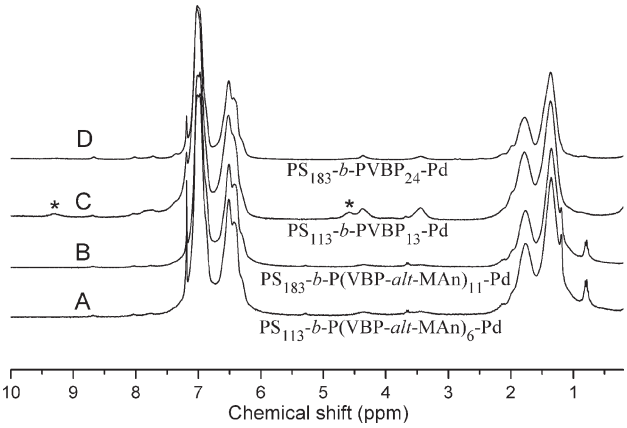


**Figure 2.** $^1$H-NMR spectra of PS-*b*-P(VBP-*alt*-MAn)-Pd and PS-*b*-PVBP-Pd in $CDCl_3$.

The number of VBP units in each chain was calculated through the relative integration ratio of the proton resonances of PS and VBP. In our calculation, the number of VBP unit of PS-*b*-P(VBP-*alt*-MAn) was assumed as the same as that of Maleci anhydride, because an alternating copolymer is preferentially obtained when the styrenic monomer is copolymerized with MAn.[38]

In the IR spectra, the ester carbonyl absorption of both PS-*b*-P(VBP-*alt*-MAn) and PS-*b*-PVBP appeared two peaks in the same locations, namely, occurred at 1742 $cm^{-1}$ and 1717 $cm^{-1}$ (Supporting Information Figure S1). It is unclear for us that ester carbonyl absorption of picolinate showed two peaks, which are different from other usual ester showing one peak. Actually, Konaka and coworkers[39] also found the two peaks of methyl picolinate appeared at 1744 $cm^{-1}$ and 1701 $cm^{-1}$, respectively. In addition, the characteristic carbonyl absorption peak of MAn was also observed at 1780 $cm^{-1}$ in the IR spectra of PS-*b*-P(VBP-*alt*-MAn) (Supporting Information Figure S1). Table I shows good agreements between GPC-determined ($M_{n,GPC}$) and theoretical molecular weight ($M_{n,th}$), and the PDIs were all narrow (<1.30). Moreover, no trace of residual macroinitiator was detected by GPC (Supporting Information Figure S2). It indicated that nearly all macroinitiators were involved in reinitiation.

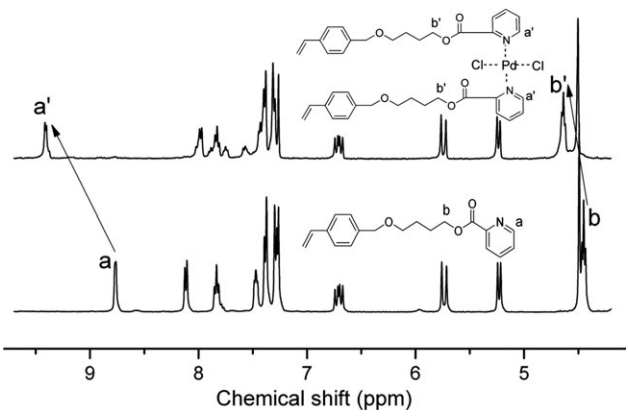


**Figure 3.** $^1$H-NMR spectra of monomer VBP and its complex with $PdCl_2$ in $CDCl_3$.

Applied Polymer SCIENCE

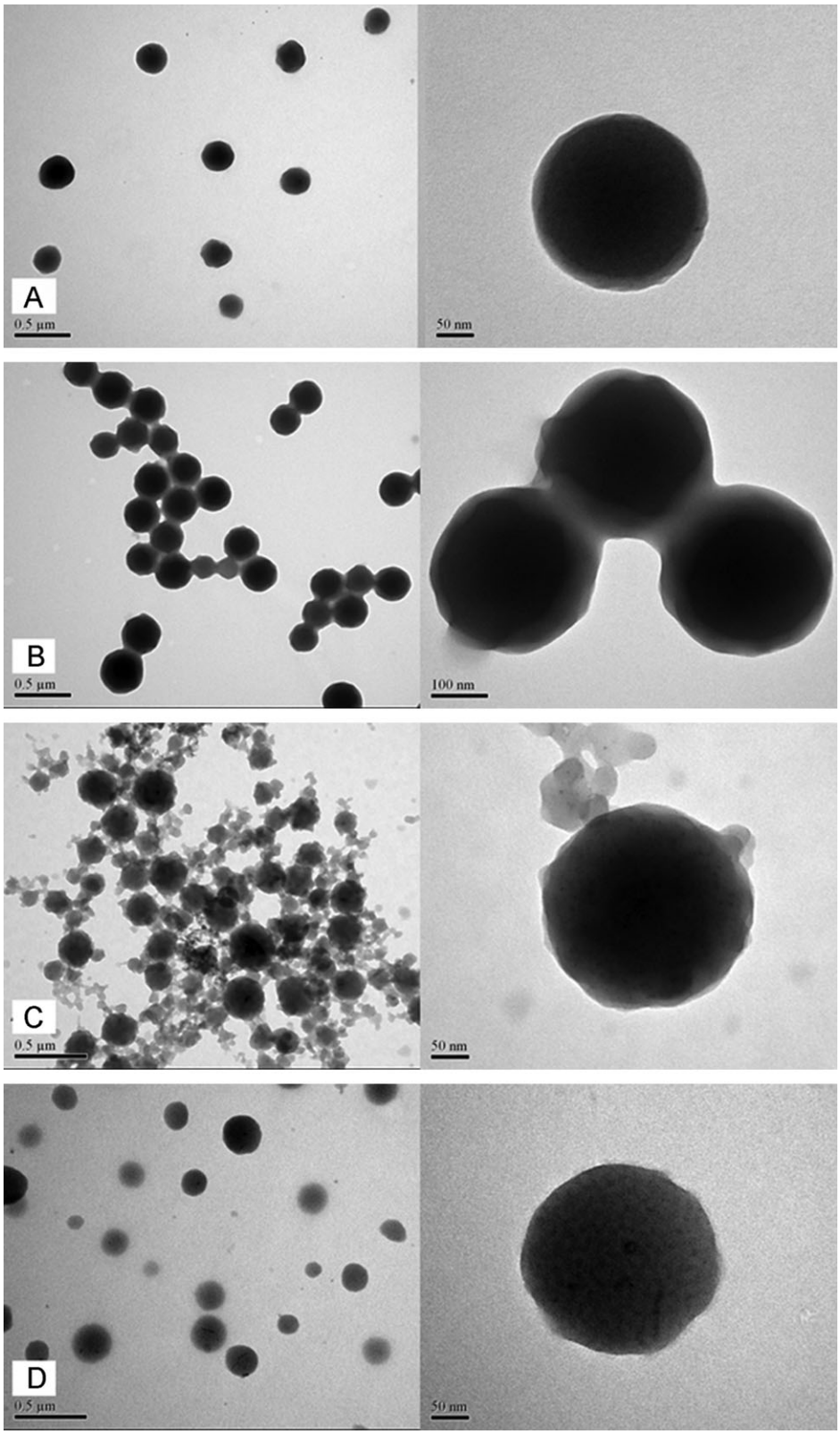


**Figure 4.** TEM images of the PS-*b*-P(VBP-*alt*-MAn)-Pd and PS-*b*-PVBP-Pd in the mixture of THF and ethanol. A, $PS_{113}$-*b*-P(VBP-*alt*-$MAn)_6$-Pd, Diameter: 340 nm; B, $PS_{183}$-*b*-P (VBP-*alt*-$MAn)_{11}$-Pd, Diameter: 300 nm; C, $PS_{113}$-*b*-$PVBP_{13}$-Pd, Diameter: 270 nm; D, $PS_{183}$-*b*-$PVBP_{24}$-Pd, Diameter: 250 nm.

### Immobilization of $PdCl_2$

To preserve the induced aggregates and further improve the protection for Pd, 1,6-diaminohexane (cross-linker) was added to cross-link with the MAn units in a 20% molar amount of MAn after the pyridine groups of the PS-*b*-P(VBP-*alt*-MAn) were coordinated with $PdCl_2$. In the $^1$H-NMR spectrum [Figure 2(A)] of cross-linked $PS_{113}$-*b*-P(VBP-*alt*-MAn)$_6$-Pd (**A**), it was found that all the signals of block P(VBP-*alt*-MAn) decreased significantly, and only a few free pyridine groups were visible. The resonance peaks of some $CH_2$ from 1,6-diaminohexane appeared at upfield. Moreover, the two absorption peaks of the ester merged together (1735 $cm^{-1}$) in the IR spectra of the $PS_{113}$-*b*-P(VBP-*alt*-MAn)$_6$-Pd (Supporting Information Figure S3). It may be ascribed to the coordination of pyridine groups with $PdCl_2$, which affected the electron density of the ester carbonyl group. Simultaneously, the intensity of MAn peaks sharply decreased compared to its precursor in the IR spectrum, which indicated that most of anhydride groups have reacted with 1,6-diaminohexane. In addition, this cross-linking should generate newly formed amide carbonyl groups (MAn + hexandiamine), whose absorption peak generally appears in the region of between 1630 and 1680 $cm^{-1}$ in IR spectrum.[40] However, amide carbonyl absorption was not observed in the IR spectrum. It may be because of the following two reasons: (1) the content of amide carbonyl groups was very low, because it was just 20% molar amount of MAn or lower on the basis of the incomplete cross-link reaction conversion; (2) ester carbonyl absorption (1735 $cm^{-1}$) is a relative broad peak and its position was overlapped with that of amide carbonyl absorption. As a matter of fact, the model reaction of 1,6-diaminohexane with MAn had been carried out at room temperature before the cross-linking reaction, and an amide carbonyl and a carboxyl acid group were generated, respectively. On the other hand, it is well known that $PdCl_2$ usually coordinates with two ligands. However, for the $PS_{113}$-*b*-P(VBP-*alt*-MAn)$_6$-Pd, it was found that the Pd loading was 0.87 wt % by inductive-coupled plasma atomic emission analysis (ICP-AES), which corresponds the molar ratio of pyridine groups to $PdCl_2$ to 4.65 : 1. As a result, the Pd contribution in the resulting polymer is slightly lower than the content of Pd added into the reaction system (pyridine/$PdCl_2$ = 4/1). It was surmised that some of Pd was lost when precipitating the immobilized Pd polymer. Besides, when the $PdCl_2$ was immobilized on a block copolymer with the higher molecular weight ($PS_{183}$-*b*-P(VBP-*alt*-MAn)$_{11}$-Pd (**B**)), the $^1$H-NMR spectrum showed a similar behavior [Figure 2(B)].

$PS_{113}$-*b*-$PVBP_{13}$-Pd (**C**) and $PS_{183}$-*b*-$PVBP_{24}$-Pd (**D**) were obtained under the same conditions except cross-linking, whose $^1$H-NMR spectra [Figure 2(C,D)] also showed similar behaviors to that of **A** and **B**. The intensity of block PVBP decreased obviously after the immobilization of $PdCl_2$, and only very weak peaks of free pyridine groups were visible. Nevertheless, in the $^1$H-NMR spectrum of **C**, the intensity of block PVBP was much stronger than that of other immobilized catalysts. In the meantime, the resonance peaks of an $H$ on the pyridine groups (from 8.77 to 9.39 ppm) and a $CH_2$ on the spacer (from 4.46 to 4.65 ppm) both shifted downfield [marked with asterisks in Figure 2(C) and more detail in Supporting Information Figure S4] after the coordination of pyridine groups with $PdCl_2$. With regard to the $PS_{113}$-*b*-$PVBP_{13}$-Pd (**C**), due to the weaker interchain interaction, the polymer was more soluble in $CDCl_3$, thus displaying the stronger resonance intensity of block PVBP compared to other three catalysts. In addition, the two absorption peaks of the ester also merged together (1735 $cm^{-1}$) in the IR spectra of the PS-*b*-PVBP-Pd when supported by Pd (Supporting Information Figure S3).

**Table II.** Suzuki-Coupling Reaction in Water Catalyzed by Catalysts **A**, **B**, **C**, and **D**[a].

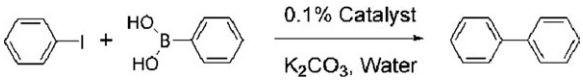


| Entry | Cat. (mol % Pd) | $T$ (°C)[b] | $t$ (h)[c] | Yield (%)[d] |
|---|---|---|---|---|
| 1 | **A** (0.1) | 80 | 20 | 92 |
| 2 | **B** (0.1) | 80 | 20 | 77 |
| 3 | **C** (0.1) | 80 | 9 | 94 |
| 4 | **D** (0.1) | 80 | 9 | 83 |

[a]Reaction conditions: iodobenzene (0.5 mmol), $PhB(OH)_2$ (0.75 mmol), $K_2CO_3$ (0.75 mmol), Pd catalyst, and $H_2O$ (2 mL), **A** ($PS_{113}$-*b*-P(VBP-*alt*-MAn)$_6$-Pd), **B** ($PS_{183}$-*b*-P(VBP-*alt*-MAn)$_{11}$-Pd), **C** ($PS_{113}$-*b*-$PVBP_{13}$-Pd), and **D** ($PS_{183}$-*b*-$PVBP_{24}$-Pd).
[b]Oil bath temperature.
[c]Where the conversion of iodobenzene reached to >99% monitored by GC at the given time in this table and the yield cannot be improved even prolonging the reaction time.
[d]Isolated yield after flash chromatography and the purity of the product was confirmed by $^1$H-NMR.

To further confirm the immobilization of $PdCl_2$, the complex of monomer VBP with $PdCl_2$ was also investigated by the use of $^1$H-NMR spectroscopy. It was observed that the chemical shift of $H^a$ (from 8.76 to 9.41 ppm) and $H^b$ (from 4.45 to 4.63 ppm) in the VBP clearly showed a downfield shift after the coordination with $PdCl_2$ in the $^1$H-NMR spectra (Figure 3). This downfield shift is consistent with that of catalyst **C**. The NMR spectrum results demonstrated that pyridine-containing monomer could easily coordinate with $PdCl_2$ in our protocol.

### Morphological Study

As far as amphiphilic diblock copolymers are concerned, one of the most interesting properties is their ability of self-assembling into a large variety of structures.[41–45] Thus, in our study, the increase of hydrophilicity of block P(VBP-*alt*-MAn) and PVBP after the coordination of pyridine groups with $PdCl_2$ may drive the formation of polymer superstructures, such as micelles, in some selective solvents. Therefore, the morphologies of the Pd catalysts (PS-*b*-P(VBP-*alt*-MAn)-Pd and PS-*b*-PVBP-Pd) were investigated in a mixed solvent of THF and ethanol by TEM. From the TEM images (Figure 4), the well-defined spherical micelles with a slightly different diameter could be observed, whose diameter was rather large and varied between 100 and 340 nm. Nevertheless, the spherical micelles of cross-linked PS-*b*-P(VBP-*alt*-MAn)-Pd were more regular than those of PS-*b*-PVBP-Pd. Moreover, the diameters of PS-*b*-P(VBP-*alt*-MAn)-Pd were obviously larger than that of PS-*b*-PVBP-Pd. This disparity in the formation of micelles may be attributed to the cross-linking action.

**Table III.** Recycling of Catalysts **A**, **C**, and **D** in Aqueous Suzuki-Coupling Reaction[a]

| Entry | Cat. (mol % Pd) | Fresh use | | 1st recycle | | 2nd recycle | | 3rd recycle | | 4th recycle | |
|---|---|---|---|---|---|---|---|---|---|---|---|
| | | *t* (h)[b] | Yield (%)[c] | *t* (h)[b] | Yield (%)[c] | *t* (h)[b] | Yield (%)[c] | *t* (h)[b] | Yield (%)[c] | *t* (h)[b] | Yield (%)[c] |
| 1 | **A** (0.1) | 20 | 92 | 20 | 88 | 20 | 82 | 20 | 84 | 20 | 85 |
| 2 | **C** (0.1) | 6 | 94 | 11 | 77 | 11 | 56 | 11 | 18 | 24 | <10 |
| 3 | **D** (0.1) | 6 | 83 | 11 | 58 | 11 | 46 | 11 | 35 | 24 | <5 |

[a]Reaction conditions: iodobenzene (0.5 mmol), $PhB(OH)_2$ (0.75 mmol), $K_2CO_3$ (0.75 mmol), Pd catalyst, and $H_2O$ (2 mL), **A** ($PS_{113}$-*b*-P(VBP-*alt*-MAn)$_6$-Pd), **C** ($PS_{113}$-*b*-$PVBP_{13}$-Pd), and **D** ($PS_{183}$-*b*-$PVBP_{24}$-Pd).
[b]Where the conversion of iodobenzene reached to >99% monitored by GC and the yield cannot be improved even prolonging the reaction time.
[c]Isolated yield after flash chromatography and the purity of the product was confirmed by $^1$H-NMR.

Upon closer inspection of the images, we could clearly distinguish between the core and the shell of the micelles based on the difference in electron density. In the $PS_{113}$-*b*-P(VBP-*alt*-MAn)$_6$-Pd (**A**) and $PS_{183}$-*b*-P(VBP-*alt*-MAn)$_{11}$-Pd (**B**), the Pd was located in the core of the micelles, whereas the Pd was immobilized on the shell of the micelles in the $PS_{113}$-*b*-$PVBP_{13}$-Pd (**C**) and $PS_{183}$-*b*-$PVBP_{24}$-Pd (**D**). It may be caused by the interchain interaction of **A** or **B** much stronger than that of **C** or **D**. Generally, hydrophilic block will take orientation toward outside (ethanol phase), when ethanol was added into the THF solution of an amphiphilic diblock copolymer.[46] However, considering **A** or **B**, the interchain interaction not only came from the cross-linking of MAn units with 1,6-diaminohexane, but also from the coordination of pyridine groups with Pd. This strong interchain interaction made it difficult for the hydrophilic block (the Pd-containing block) to take orientation toward outside (ethanol phase). The hydrophilic block has to take orientation toward inside and assemble into the core of the micelles. In the case of **C** or **D**, the interchain interaction just came from the coordination of pyridine groups with Pd. Hence, this relatively weak interchain interaction could hardly affect the hydrophilic block (the Pd-containing block) taking orientation toward outside when adding the ethanol into the THF solution of **C** or **D**. The Pd-containing block assembled into the shell of the micelles.[25] In addition, the diameters of micelles decreased from **A** and **C** to **B** and **D**, respectively. It was speculated that the interchain interaction was strengthened with the increase of hydrophilic block length and further led to the shrinkage of micelles. Moreover, the increase of PS chain length from **A** to **B** also resulted in an obvious increase of shell wall thickness.

### Evaluation of Catalytic Performance

With the aim at evaluating the catalytic ability and the recyclability of these immobilized Pd catalysts, we herein adopted the heterogeneous Suzuki-coupling reaction[47] of iodobenzene and phenylboronic acid in water as a model reaction. Under the standard reaction condition ($K_2CO_3$ as base, 80°C), the catalytic performances of **A–D** with 0.1 mol % were examined. GC was herein just used to detect the ending of reaction. When the conversion of iodobenzene reached to >99%, the reaction was quenched. The results were summarized in Table II. It was found that both **A** and **C** showed the higher catalytic activity than that of **B** and **D**, respectively. It demonstrated that the long PS chain is negative for the Pd catalytic activity whether cross-linking or not. In addition, the catalytic activity of **C** and **D** was slightly higher than that of **A** and **B**, respectively, possibly due to the easier access to the active sites of the immobilized Pd catalyst on the outer shell of the micelles.[48]

As an important research point, the recycle of catalysts **A**, **C**, and **D** in the Suzuki reaction was further examined under the same conditions, and the results were listed in Table III. It could be found that the catalytic activities of **C** and **D** decreased sharply with the increase in the recycle times. However, the catalytic activity of **A** could be maintained even after four recycles. To test if the Pd leaching from the solid catalyst during reaction and well understand the difference of the catalytic activity of **A** and **C** in the recycling, the aqueous phase reaction mixture was collected after the completion of the coupling reaction, and the Pd content in aqueous phase was investigated by the use of ICP-AES analysis. Expectedly, it was found that the total Pd content in water after four recycles corresponds to only 2.31% of the initial Pd content of catalyst **A**, whereas, for the catalyst **C**, the total Pd content in water reached to 34.37% after four recycles. This result strongly suggested the cross-linking plays a crucial role in the capture of $Pd^{2+}$ during the coupling reaction, and the cross-linking structure in catalyst **A** effectively prohibits the leaching of the Pd. In our study, the micelles of catalyst just act as the nanoreactor, and the substrates can diffuse into the core or shell of the micelles. If the Pd leaches from the supports, the catalyst will become unstable and thus lose activity. Nevertheless, it does not indicate the corresponding change of the Pd's valence state. So, the Pd leaching from supports into water is responsible for the fast deactivation of the catalysts. Consequently, we concluded that the cross-linking is an effective strategy to keep micelles supported Pd catalyst's activity and enhance its durability simultaneously in the recycle.

## CONCLUSION

In the present study, the morphologies, catalytic activity, and recyclability of two various immobilized Pd catalysts were investigated. It was concluded that the cross-linking between 1,6-diaminohexane and MAn had a significant effect on the morphology of the Pd catalyst in the selective solvents, especially, affecting the location of the Pd in the micelles. More importantly, the catalytic activity of Pd catalysts with cross-linking structure could be maintained better during the catalytic recycling compared to non-cross-linking counterparts. Thereby, the cross-linking strategy is superior to those presently known in

terms of both keeping efficiency and the ease of separation and recycling of the catalyst.

## ACKNOWLEDGMENTS

We acknowledge the financial support from the National Natural Science Foundation of China (21072099) for this work.

## REFERENCES


1. Tsuji, J. Palladium Reagents and Catalysts; Wiley: Chichester, **1995.**
2. Li, C.-J.; Chen, L. *Chem. Soc. Rev.* **2006,** *35*, 68.
3. Eliasa, S.; Vigaloka, A. *Adv. Synth. Catal.* **2009,** *351*, 1499.
4. Yin, L.; Liebscher, J. *Chem. Rev.* **2007,** *107*, 133.
5. Leadbeater, N. E.; Marco, M. *Chem. Rev.* **2002,** *102*, 3217.
6. Mitsudome, T.; Nose, K.; Mori, K.; Mizugaki, T.; Ebitani, K.; Jitsukawa, K.; Kaneda, K. *Angew. Chem. Int. Ed.* **2007,** *46*, 3288.
7. Heckel, A.; Seebach, D. *Angew. Chem. Int. Ed.* **2000,** *39*, 165.
8. Shi, X.; Han, X.; Ma, W.; Fan, J.; Wei, J. *Appl. Organometal. Chem.* **2012,** *26*, 16.
9. Jana, S.; Dutta, B.; Bera, R.; Koner, S. *Inorg. Chem.* **2008,** *47*, 5512.
10. Jana, S.; Haldar, S.; Koner, S. *Tetrahedron Lett.* **2009,** *50*, 4820.
11. Bhunia, S.; Sen, R.; Koner, S. *Inorg. Chim. Acta* **2010,** *363*, 3993.
12. Schauermann, S.; Hoffmann, J.; Johanek, V.; Hartmann, J.; Libuda, J.; Freund, H.-J. *Angew. Chem., Int. Ed.* **2002,** *41*, 2532.
13. Riahi, G.; Guillemot, D.; Polisset-Tfoin, M.; Khodadadi, A. A.; Fraissard, J. *Catal. Today* **2002,** *72*, 115.
14. Uozumi, Y.; Nakao, R. *Angew. Chem. Int. Ed.* **2003,** *42*, 194.
15. Ogasawara, S.; Kato, S. *J. Am. Chem. Soc.* **2010,** *132*, 4608.
16. Beletskaya, I. P.; Kashin, A. N.; Litvinov, A. E.; Tyurin, V. S.; Valetsky, P. M.; Van Koten, G. *Organometallics* **2006,** *25*, 154.
17. Karimi, B.; Akhavan, P. F. *Chem. Commun.* **2009,** 3750.
18. Grandsirea, A. F.; Labordeb, C.; Lamatyb, F.; Mehdia, A. *Appl. Organometal. Chem.* **2010,** *24*, 179.
19. Liu, Y. X.; Ma, Z. W.; Jia, J.; Wang, C. C.; Huang, M. L.; Tao, J. C. *Appl. Organometal. Chem.* **2010,** *24*, 646.
20. Moad, G.; Rizzardo, E.; Thang, S. H. *Aust. J. Chem.* **2005,** *58*, 379.
21. Matyjaszewski, K.; Xia, J. H. *Chem. Rev.* **2001,** *101*, 2921.
22. Kamigaito, M.; Ando, T.; Sawamoto, M. *Chem. Rev.* **2001,** *101*, 3689.
23. Hawker, C. J.; Wooley, K. L. *Science* **2005,** *309*, 1200.
24. Brayner, R.; Viau, G.; Bozon-Verduraz, F. *J. Mol. Catal. A: Chem.* **2002,** *182–183*, 227.
25. Chernyshov, D. M.; Bronstein, L. M.; Börner, H.; Berton, B.; Antonietti, M. *Chem. Mater.* **2000,** *12*, 114.
26. Zhang, M.; Zhang, W.; Wang, S. *J. Phys. Chem. C* **2010,** *14*, 15640.
27. Klingelhöfer, S.; Heitz, W.; Greiner, A.; Oestreich, S.; Förster, S.; Antonietti, M. *J. Am. Chem. Soc.* **1997,** *119*, 10116.
28. Jiang, X.; Wei, G.; Zhang, X.; Zhang, W.; Zheng, P.; Wen, F.; Shi, L. *J. Mol. Catal. A: Chem.* **2007,** *277*, 102.
29. Azzam, T.; Bronstein, L.; Eisenberg, A. *Langmuir* **2008,** *24*, 6521.
30. Bronstein, L.; Chernyshov, D. M.; Volkov, I. O.; Ezernitskaya, M. G.; Valetsky, P. M.; Matveeva, V. G.; Sulmanz, E. M. *J. Catal.* **2000,** *196*, 302.
31. Seregina, M. V.; Bronstein, L. M.; Platonova, O. A.; Chernyshov, D. M.; Valetsky, P. M.; Hartmann, J.; Wenz, E.; Antonietti, M. *Chem. Mater.* **1997,** *9*, 923.
32. Semagina, N. V.; Bykov, A. V.; Sulman, E. M.; Matveeva, V. G.; Sidorov, S. N.; Dubrovina, L. V.; Valetsky, P. M.; Kiselyova, O. I.; Khokhlov, A. R.; Stein, B.; Bronstein, L. *J. Mol. Catal. A: Chem* **2004,** *208*, 273.
33. Schönfelder, D.; Nuyken, O.; Weberskirch, R. *J. Organomet. Chem.* **2005,** *690*, 4648.
34. Zheng, P.; Zhang, W. *J. Catal.* **2007,** *250*, 324.
35. Jiang, X.; Wang, Y.; Zhang, W.; Zheng, P.; Shi, L. *Macromol. Rapid Commun.* **2006,** *27*, 1833.
36. Vosloo, J. J.; De Wet-Roos, D.; Tonge, M. P.; Sanderson, R. D. *Macromolecules* **2002,** *35*, 4894.
37. Takenaka, Y.; Ito, H.; Hasegawa, M.; Iguchi, K. *Tetrahedron* **2006,** *62*, 3380.
38. Seymour, R. B.; Garner, D. P. *Polymer* **1976,** *17*, 21.
39. Kiyono, H.; Tatsunami, R.; Kurai, T.; Takeuchi, H.; Egawa, T.; Konaka, S. *J. Phys. Chem. A* **1998,** *102*, 1405.
40. Brown, W. H.; Foote, C. S.; Iverson, B. L.; Anslyn, E. Organic Chemistry; Brooks/Cole: Belmont, CA; Cengage Earning, 6th ed., **2012.**
41. Discher, D. E.; Eisenberg, A. *Polym. Vesicles Science* **2002,** *297*, 967.
42. Jain, S.; Bates, F. S. *Science* **2003,** *300*, 460.
43. Zhou, Y. F.; Yan, D. Y. *Angew. Chem. Int. Ed.* **2005,** *44*, 3223.
44. Koide, A.; Kishimura, A.; Osada, K.; Jang, W. D.; Yamasaki, Y.; Kataoka, K. *J. Am. Chem. Soc.* **2006,** *128*, 5988.
45. Kotsuchibashi, Y.; Ebara, M.; Yamamoto, K.; Aoyagi, T. *J. Polym. Sci. Part A: Polym. Chem.* **2010,** *48*, 4393.
46. Moughton, A. O.; O'Reilly, R. K. *J. Am. Chem. Soc.* **2008,** *130*, 8714.
47. Miyaura, N.; Suzuki, A. *Chem. Commun.* **1979, 866.**
48. Zhang, M.; Zhang, W. *J. Phys. Chem. C* **2008,** *112*, 6245.